Luminescence spectra and crystal field analysis of LaOBr doped with Tm^{3+}

1994 J. Phys.: Condens. Matter 6 2031

(http://iopscience.iop.org/0953-8984/6/10/020)

J. Phys.: Condens. Matter 6 (1994) 2031–2037. Printed in the UK

Luminescence spectra and crystal field analysis of LaOBr doped with Tm^{3+}

Z Mazurak†, A Garcia‡ and C Fouassier‡

† Department of Solid-State Physics, Polish Academy of Sciences, Wandy Street 3, PL-41-800 Zabrze, Poland

‡ Laboratoire de Chimie du Solide du CNRS, Université de Bordeaux 1, F-33405 Talence Cédex, France

Received 1 February 1993, in final form 11 October 1993

Abstract. Crystal-field parameters ($B_{k,m}$) were obtained for LaOBr doped with Tm^{3+} from the analysis of luminescence spectra. The crystal-field Hamiltonian $H_{CEF} = \sum_{km} B_{km}^{+} \sum_{i} C_{km}(\hat{r}_i)$ for the C_{4v} symmetry comprises five non-zero $B_{k,m}$ parameters. The results of model crystal-field calculations in C_{4v} symmetry for Tm^{3+} in LaOBr are compared with experimental data, for the lowest ten $[S, L]J$ states $4f^{12}$ configuration. The set of crystal-field parameters (CFPs) calculated on the basis set of 54 sublevels reproduced the experimental level scheme within an RMS deviation of 11 cm^{-1}.

1. Introduction

The PbFCl-type phosphors activated with rare-earth ions have received considerable scientific and industrial attention. REOCl-type compounds have long been used as hosts for a variety of activators. Brixner and co-workers [1] introduced ions such as Sm^{3+}, Eu^{3+}, Tb^{3+} and Dy^{3+} into LaOCl and LuOCl hosts and the luminescence was discussed as a function of the local site symmetry. Rare-earth oxyhalides, REOX, where X = Cl, Br, activated with Eu^{2+} and Tb^{3+} ions, are used as x-ray intensifying phosphors. Recently a crystal-field analysis was conducted on Eu^{3+}- and Tb^{3+}-doped LaOCl [2]. The spectroscopic data for the LaOCl:Pr^{3+} system has been published by us [3]. In the present work the study of luminescence spectra and crystal-field effects in the oxyhalide series is extended to the LaOBr:Tm^{3+} system.

2. Structure of RE^{3+} oxybromides

Unlike the corresponding oxychloride series, the whole RE^{3+} oxybromide series has tetragonal PbFCl structure (space group $P4/nmm$—D_{4h}^{7}, $z = 2$), with layers of complex cations $(LnO)_n^{n+}$ alternating with halide layers. The RE^{3+} atoms are coordinated to four oxygen and four halogen atoms with C_{4v} point site symmetry. Unit-cell dimensions and atomic distances in LaOBr are as follows: $a = 0.4145$ nm; $c = 0.7359$ nm; La–O, 0.229 nm; La–Br, 0.328 nm and La–Br′, 0.347 nm [4].

0953-8984/94/102031+07$19.50

3. Experimental details

Powder samples of LaOBr doped with Tm^{3+} in nominal molar concentration 2% were obtained by dissolving the rare-earth oxides (Rhône–Poulenc 99.999%) in HBr (Baker), evaporating to dryness, and firing under N_2 at 700 °C for 6 h. The resulting products had a white colour. The samples were checked by x-ray powder diffraction.

A number of general luminescence measurements was performed using a Jobin–Ivon spectrofluorimeter. The output was stored by an IBM-XT microcomputer. The temperature of the samples could be regulated between 4.2 K and room temperature using a liquid He cryostat with a temperature controller.

The crystal-field calculations were carried out on the basis of the 31 $^{2S+1}L_J$ Stark levels. The diagonalization of the 54 × 54 energy-level matrix gave the eigenvalues and eigenfunctions where the J mixing was taken into account.

4. Analysis of the LaOBr:Tm^{3+} spectra

The Tm^{3+} ions replace the La^{3+} host cations in LaOBr in a crystallographic point site of C_{4v} symmetry, for which the free ion $^{2S+1}L_J$ levels split into Stark components. The number of crystal-field components result from the combination of the J value with the crystallographic point symmetry of the rare-earth ion site in the crystal. Splitting of the $^{2S+1}L_J$ (J = 0, 1, ..., 6) levels are presented in table 1 for the C_{4v} symmetry.

Table 1. Splitting of the $^{2S+1}L_J$ levels for the C_{4v} symmetry.

	J						
Γ	0	1	2	3	4	5	6
A_1	1	—	1	—	2	1	2
A_2	—	1	—	1	1	2	1
B_1	—	—	1	1	1	1	2
B_2	—	—	1	1	1	1	2
E	—	1	1	2	2	3	3

4.1. Excitation spectrum

The excitation spectrum (λ_{emi} = 459.7 nm) recorded at liquid helium temperature (LHeT) (see figure 1) shows a strong sharp peak near 28 000 cm^{-1} and a wide band above 42 000 cm^{-1}. The wide band is due to the excitation from the $^3H_6$ ground level to charge transfer states (CTSs); the sharp peaks correspond to transitions within the $4f^{12}$ configuration. The peaks near 28 000 cm^{-1} were assigned to transitions from the $^3H_6$ ground level to the $^1D_2$ level on the basis of the characteristic splittings and energy positions of these peaks. The data were used to calculate the energies of $^1D_2$ and $^3H_6$ sublevels.

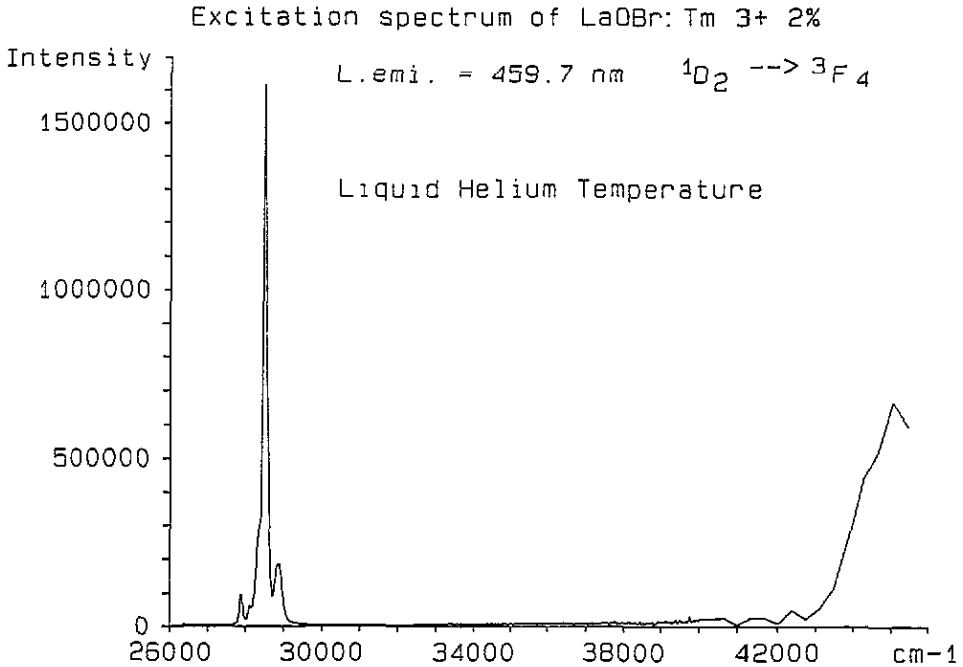

Figure 1. LHeT excitation spectrum of LaOBr:Tm^{3+} 2 mol% (λ_{emi} = 459.7 nm, transition $^1D_2 \rightarrow {}^3F_4$).

4.2. Emission spectra

The total number of allowed $^1D_2 \rightarrow {}^3H_{4,5,6}$, $^3F_{2,3,4}$ transitions is quite high, over 100 lines, because of the degeneracy of the emitting $^1D_2$ level. At ambient temperature all of these transitions should be present and even at 77 K the spectra are complicated, with several overlapping lines. The thermal population of upper crystal-field components of the $^1D_2$ level is greatly reduced at 4.2 K and as consequence only a few lines are observed in the 4.2 K spectra. The room-temperature emission spectrum of 2 mol% Tm^{3+} in LaOBr, excited at 353.2 nm, is shown in figure 2 as a representative example. Under excitation at 353.2 nm, electrons in the ground state $^3H_6$ are first excited to the $^1D_2$ level and then partly relaxed to the $^1G_4$ level. Transitions from $^1D_2$ to lower levels were assigned to $^1D_2 \rightarrow {}^3H_{4,5,6}$, $^3F_{2,3,4}$. Other lines originate from $^1G_4 \rightarrow {}^3H_6$ transitions, which are mainly of electric-dipole character. Transitions from the $^1D_2$ level to $^3H_5$ state are the most intense, giving the phosphors a blue colour. The Tm^{3+} luminescence from $^3H_{4,5}$ levels is located in the region of 1660 and 1890 nm and were not observed by us, because it was out of the range of our detection system.

The 4.2 K emission spectrum of 2 mol% Tm^{3+} in LaOBr, excited at 353.2 nm consists of several narrow peaks attributed to the $^1D_2 \rightarrow {}^3H_{4,5,6}$, $^3F_{2,3,4}$ transitions. The intensity of the $^1D_2 \rightarrow {}^3F_4$ emission is relatively weak compared to the $^1D_2 \rightarrow {}^3H_5$ luminescence intensity. The number of emission lines observed for the separate transitions is equal to or less than the number of lines expected for the Stark splitting in a single site with symmetry C_{4v}. The derived energy levels of Tm^{3+} in the LaOBr host is given in table 3, 'experimental' column. These are calculated using the emission lines at room temperature and 4.2 K. The ground Stark level A_1 of $^3H_6$ is well isolated; the next highest one lies 49 cm^{-1} above. The energy of 31 Stark levels was determined for the LaOBr:Tm^{3+} compound.

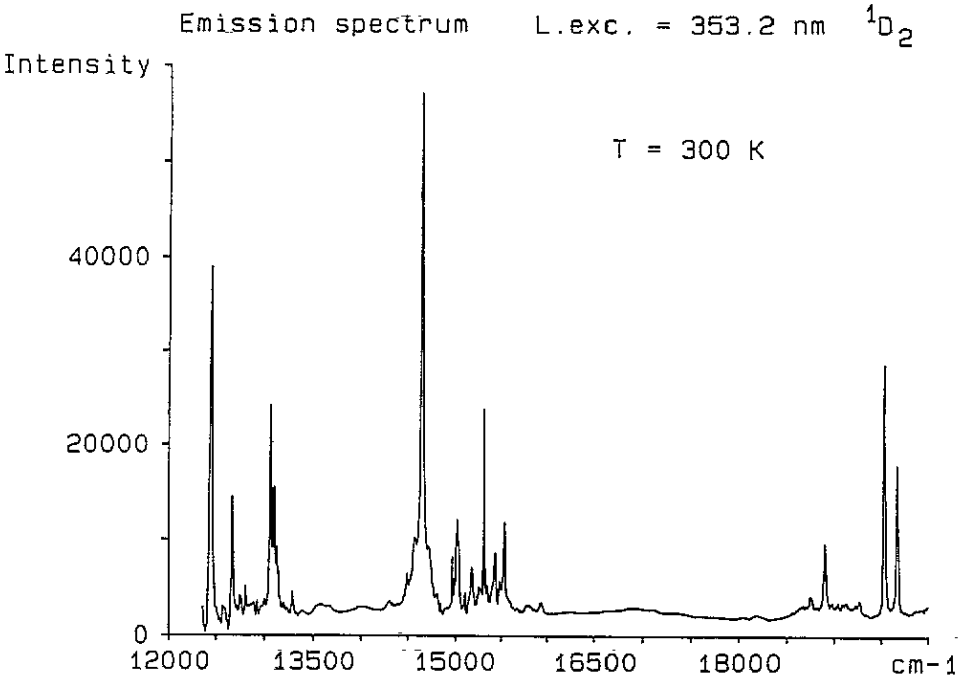

Figure 2. Room-temperature emission spectrum of 2 mol% Tm^{3+} in LaOBr (λ_{exc} = 353.2 nm via the $^1D_2$ state).

5. Crystal-field calculation

The point-group symmetry of the rare-earth oxybromides is C_{4v} [4]. In our crystal-field analysis, we take a crystal-field Hamiltonian, in the irreducible tensor form

$$H_{CEF} = \sum_{km} B^+_{km} \sum_i C_{km}(\hat{r}_i) \tag{1}$$

where B^+_{km} are crystal-field parameters (+ denotes a complex conjugate) and where C_{km} are spherical tensors, related to ordinary spherical harmonics $Y(\Theta_i \Phi_i)$ by

$$C_{km}(\hat{r}_i) = (4\pi/(2k+1))^{1/2} Y_{km}(\Theta_i, \Phi_i) \tag{2}$$

where Θ_i and Φ_i are polar coordinates of the ith electron.

Symmetry considerations have a profound effect on interpretation of the spectra of rare-earth ions. We have already mentioned the effect of symmetry on selection rules for electric- and magnetic-dipole transitions and on the classification of crystal-field-split energy levels.

Invariance under the point-group operations requires that the crystal-field Hamiltonian only contains operators that transform as the identity representation of the point group. Except for the cubic groups, these operators are generally easy to determine; all group operators may be constructed from the following operators: (a) n-fold rotation about z, $R_z(2\pi/n)$; (b) coordination inversion, I; (c) twofold rotation about x, $R_x(\pi)$.

It can be easily shown that the C_{km} transform under these operations as follows:

$$R_x(2\pi/n)C_{km} = \exp(-2\pi i m/n)C_{km} \tag{3}$$

$$IC_{km} = (-1)^k C_{km} \tag{4}$$

$$R_x(\pi)C_{km} = (-1)^k C_{k-m}. \tag{5}$$

Table 2. The crystal-field parameters $B_{k,m}$ in cm^{-1} for Tm^{3+}-doped LaOBr (point group C_{4v}), YPO_4 (point group D_{2d}) and YVO_4 (point group D_{2d}).

$B_{k,m}$	LaOBr	YPO_4 [10]	YVO_4 [10]
B_{20}	−124	275	−132
B_{40}	335	6	377
B_{44}	850	692	898
B_{60}	−522	−644	−521
B_{64}	− 46	55	− 52
RMS	11	24	25

Further, since H_{CEF}, when acting between $4f^N$ states, connects two states of the same parity, odd-parity terms in H_{CEF} drop out, and from (3), k must be even. In addition C_{km} is an irreducible tensor that connects single-electron states with $l = 3$; therefore, by the triangular inequalities, we must have $0 \leqslant k \leqslant 6$. These considerations are sufficient to determine which $B_{k,m}$ are non-vanishing for all point-group groups.

In our crystal-field analysis, we assume a crystal-field Hamiltonian C_{4v}. It has been recognized that the crystal-field parameters, $B_{k,m}$, can all be chosen real for C_{4v} symmetry. The resulting Hamiltonian given by (1) results in five independent parameters and is written

$$H_{CEF} = B_{2,0}C_{2,0} + B_{4,0}C_{4,0} + B_{44}\left(C_{4,-4} + C_{4,4}\right) + B_{6,0}C_{6,0} + B_{6,4}\left(C_{6,-4} + C_{6,4}\right). \tag{6}$$

The crystal-field Hamiltonian is diagonalized together with an effective free-ion Hamiltonian of the form

$$H_{free} = \sum_{[S,L]J} \Delta_{[S,L]J} |[S, L]J\rangle\langle[S, L]J| \tag{7}$$

where the sum on $[S, L]J$, in general, runs over of the lowest states of the $4f^N$ configuration. The quantities $\Delta_{[S,L]J}$ are centroid parameters, which would be equal to the experimental centres of gravity of the crystal-field-split levels if effects of J mixing by the crystal field were neglected. By diagonalizing the sum of (6) and (7), we include the major effect of J mixing. We include the lowest 10 $[S, L]J$ states in our calculations for Tm^{3+}.

Matrix elements of the crystal-field Hamiltonian are obtained from wavefunctions associated with the intermediate-coupling diagonalization of a free-ion Hamiltonian consisting of Coulomb, spin–orbit and configuration interactions. Parameter values for this free-ion Hamiltonian are those appropriate for rare-earth ions in aqueous solution [5]. The procedure used in these calculations has been described previously by Morrison *et al* [6]. The same procedure was used for our calculations of crystal-field parameters of RE^{3+} ions (RE^{3+} = Pr, Nd, Er, Tm) in $LiREP_4O_{12}$ crystals [7, 8].

The first step in our analysis of the Tm^{3+} ion in LaOBr was to obtain starting values for $B_{k,m}$ by means of point-charge lattice sums A_{km}. These are related to $B_{k,m}$ by

$$B_{k,m} = \rho_k A_{km} \tag{8}$$

where

$$\rho_k = \tau^{-k}\langle r^k\rangle_{HF}\left(1 - \sigma_k\right) \tag{9}$$

and where τ is a host-independent, ion-dependent radial expansion parameter, $\langle r^k\rangle_{HF}$ are Hartree–Fock expansion values and σ_k are shielding factors.

Crystal-field parameters for Tm^{3+} were determined by starting with $B_{k,m}$ given by (8) and varying the $B_{k,m}$ and the $\Delta_{[S,L]J}$ simultaneously until a minimum RMS deviation between calculated and experimental energy levels was found. The best-fit $B_{k,m}$ are presented in table 2 together with the corresponding RMS deviation.

The values of the RMS deviation in table 2, 11 cm^{-1}, is smaller than values obtained for the same ion in YPO_4 [9] and YVO_4 [10] (YVO_4 and YPO_4 also have RE^{3+} ions in tetragonal symmetry). The comparison of the $B_{k,m}$ values of Tm^{3+} ion in isomorphous host lattices show different B_{20} values in LaOBr and YPO_4. In accordance with crystal-field theory, phenomenological crystal-field parameters $B_{k,m}$ are written as a product $B_{k,m} = A_{k,m}\langle r^k\rangle$. The $\langle r^2\rangle$ values are strongly influenced by screening effects and, as a result, the B_{20} values should differ only slightly from one host to another.

Detailed comparisons of the calculated and experimental energy levels are given in table 3. In this table, states are identified by the maximum component in the free-ion wavefunctions. The theoretical energy levels are calculated by means of the crystal-field parameters of table 2.

Table 3. Calculated and experimental energy levels for Tm^{3+} in LaOBr, C_{4v} site; total of 31 experimental levels. RMS deviation, 11 cm^{-1}.

State	Stark	Energy (cm^{-1})		State	Stark	Energy (cm^{-1})	
$[S, L]J$	level	Experimental	Calculated	$[S, L]J$	level	Experimental	Calculated
$^3H_6$	A_1	0	0	$^3H_4$	A_1	12565	12578
	E	49	48		E	—	12612
	B_2	105	114		A_2	12612	12614
	B_1	118	127		A_1	—	12704
	E	—	155	$^3F_3$	B_1	14398	14391
	A_2	—	188		B_2	14426	14420
	A_1	—	205		E	14439	14437
	B_1	—	290		E	14448	14442
	B)2	—	305		A_2	—	14454
	E	—	332	$^3F_2$	B_2	15073	15080
$^3F_4$	B_1	—	5522		A_1	—	15102
	B_2	5615	5613		B_1	15201	15209
	E	5694	5701		E	15211	15220
	A_1	—	5742	$^1G_4$	B_1	21554	21562
	E	5795	5799		B_2	21734	21745
	A_2	—	5824		E	—	21760
	A_1	5840	5847		A_1	—	21922
$^3H_5$	A_2	8098	8105		E	—	21940
	E	8130	8131		A_2	21950	21952
	B_2	8170	8180		A_1	—	21970
	A_1	8213	8206	$^1D_2$	B_2	27789	27782
	A_2	8231	8244		A_1	27835	27839
	E	8384	8392		B_1	27885	27885
	B_1	—	8417		E	—	27904
	E	—	8430	$^3P_0$	A_1	33530	33522
$^3H_4$	B_1	—	12455	$^3P_1$	A_2	—	35920
	B_2	12480	12491		E	—	36160
	E	—	12557				

Examination of the model crystal field for the $^3F_4$ state revealed good correlation with the transitions observed. The structure observed in the energy range of the $^3F_4$ group was complex but the model calculation provided the basis for a tentative interpretation; much of the observed structure at RT had to be vibronic in origin. The broad band structure observed in the $^3F_4$ group is also observed in the $^3H_5$ group and similar considerations underlie the suggested interpretations in the two groups.

In the $^1G_4$ state we did not determine four sublevels from experiment. Experimentally, the region from about 12 500 cm^{-1} to 13 300 cm^{-1} ($^1G_4 \rightarrow {}^3H_5$ transition) contains much weak unresolved structure, which is probably vibronic, and two intensive peaks attributed to components of $^1G_4$.

6. Conclusions

With this paper we have extended the analysis of rare-earth ions in the C_{4v} sites of LaOBr. This paper has reported for the first time, excitation and luminescence spectra of Tm^{3+} in LaOBr. These spectra have been analysed with a crystal-field Hamiltonian of C_{4v} symmetry including the J-mixing effect. Crystal-field parameters in this Hamiltonian that minimize the RMS deviation between calculated and experimental energy levels have been determined. We conclude that the model calculations in the C_{4v} symmetry for Tm^{3+} in LaOBr are in good correlation with data.

Acknowledgments

The authors are indebted to Mr F Guillen for his help in measuring the emission and excitation spectra. The investigations were supported by the French Ministry of Science and Technology.

References

[1] Brixner L H, Ackerman J F and Foris C M 1991 *J. Lumin.* **26** 1
[2] Hölsä J and Porcher P 1981 *J. Chem. Phys.* **75** 2108
[3] Mazurak Z, van Vliet J P M and Blasse G 1987 *J. Solid State Chem.* **68** 227
[4] Brown D 1968 *Halides of Lanthanides and Actinides* (New York: Wiley)
[5] Carnall W T, Fields P R and Rajnak K 1968 *J. Chem. Phys.* **49** 4412, 4424, 4443, 4447, 4450
[6] Morrison C A, Leavitt R P and Wortman D E 1980 *J. Chem. Phys.* **73** 2580
[7] Mazurak Z and Gruber J B 1992 *J. Phys.: Condens. Matter* **4** 3453
[8] Mazurak Z 1992 *J. Phys.: Condens. Matter* **4** 8585
[9] Knoll K D 1971 *Phys. Status Solidi* b **45** 553
[10] Morrison C A and Leavitt R P 1982 *Handbook on the Physics and Chemistry of Rare-Earths* ed K A Gschneider Jr and L Eyring (Amsterdam: North-Holland) ch 46